

Wavelength selection in Bénard-Marangoni convection

P. Cerisier, C. Perez-Garcia,* C. Jamond, and J. Pantaloni

Systèmes Énergétiques et Transferts Thermiques, Université de Provence 13397 Marseille Cedex 13, France

(Received 18 November 1985; revised manuscript received 7 July 1986)

The influence of the vessel form, the aspect ratio Γ , and the heating gradient on the wavelength-selection mechanism in a hexagonal pattern, corresponding to Bénard-Marangoni convection, are studied experimentally. The pattern changes in an almost continuous way and shows a wavelength increase when Γ becomes greater. The wavelengths for a container where $\Gamma > 70$ and for an infinite extended layer are nearly identical.

I. INTRODUCTION

Wavelength selection in dissipative structures is a problem of great interest, which has been solved only in some cases. In recent years, much research has been devoted to it, especially in Rayleigh-Bénard (RB) convection and Belousov-Zhabotinsky reaction.¹ The RB problem deals with a shallow horizontal pool of liquid contained between rigid boundaries and heated from below. When slightly heated, the fluid remains at rest, but when a critical heating is reached, convective motions start. These motions form a structured pattern that in most cases is a pattern of rolls parallel to the shorter side of the vessel. Buoyancy forces create this instability mechanism.²

When the upper surface of the liquid pool is free, surface-tension variations with temperature also act as a destabilizing mechanism. Then, as shown theoretically by Nield,³ convective motions occur because of buoyancy and surface-tension forces. In this particular case, known as Bénard-Marangoni (BM) instability, convective motions form a hexagonal pattern.⁴

Although some defects always exist, roll and hexagonal patterns can be characterized, because of their regularity, by a wave number k (similar to that of a crystalline structure). A first idea of its value is obtained when applying the normal-mode expansion to the linearized set of equations describing the corresponding instability.² This makes it possible to obtain the so-called critical wave number k and the Rayleigh (R) and the Marangoni (M) numbers. (These nondimensional numbers R and M are not independent. Their definition and the relation between them can be found in Ref. 5.) The values of those critical numbers are obtained from the minimum of the marginal stability curve.² Beyond this critical point, weakly nonlinear analysis shows that a finite bandwidth of possible wave numbers k (or wavelength $\lambda = 2\pi/k$) exists.

For RB convection numerical calculations made by Busse and co-workers give the stability region in the R , P (the Prandtl number), and k parameter space.⁶ This region has the form of a duck head (see Fig. 19 in Ref. 7). It is limited by several kinds of instabilities (cross-roll, zig-zag, oscillatory, etc.) that have been observed and classified by Busse and Whitehead⁸ who used a shadowgraph

technique that enables a definite wavelength to be imposed.

Schlüter *et al.*⁹ studied the stability of a roll pattern in RB convection. In the case of a fluid enclosed in a container with an infinite horizontal extent, they concluded that a finite bandwidth of wave numbers proportional to $(R - R_C)^{0.5}$ is stable. Segel¹⁰ reached the same conclusion. However, following a similar analysis, Cross¹¹ and Pomeau and Manneville¹² showed that in finite vessels the interval of stable wave numbers reduces to a band proportional to $(R - R_C)$.

Koschmieder,¹³ in a review paper, quoted experimental results on wavelength variations as a function of the distance to the threshold $\epsilon = (R - R_C)/R_C$ in spontaneous (nonforced) roll patterns. Taking into consideration several liquids with a high P ($P \geq 350$), he concluded that the dimensionless wavelength λ increases with ϵ in all cases. For small ϵ , λ increases linearly. In some experiments this linear range rises to $5R_C$. The slope is different in each experiment but its average value is $(1 \pm 0.2) \times 10^{-1} \text{ K}^{-1}$. More recently, Martinet *et al.*¹⁴ have published results about the wavelength-selection problem in RB convection in air, which has a very low P ($P = 0.71$). They also observe that λ increases linearly with ϵ until it reaches a saturation limit. These results are similar for several aspect ratios and only the saturation limit changes slightly. Croquette and Pocheau¹⁵ studied the evolution of a dislocation in a forced roll pattern, and observed that this evolution always tends to an increase of λ with ϵ . The same conclusion follows from works by Ahlers *et al.*¹⁶ and Kolodner *et al.*¹⁷ Those experiments suggest that the obtained dispersion in the data is not due primarily to experimental uncertainties, but mainly to initial conditions, to the nature of walls, to the vessel form, to the aspect ratio [the ratio between the lateral length L_x or L_y and the liquid depth ($\Gamma_x = L_x/d$, $\Gamma_y = L_y/d$)], and to the Prandtl number P . Often hysteresis of changes between possible wave numbers is observed.¹⁴⁻¹⁷

It is more difficult to obtain experimental or theoretical results on BM convection because it involves a more complex instability mechanism. Therefore, the mathematical problem is also more complicated. Experiments showed that a hexagonal pattern spontaneously develops, and weakly nonlinear analysis makes it possible to determine

TABLE I. Characteristics of hexagonal containers. l is the side length of the hexagon, Γ is the aspect ratio (corresponding to a layer depth 0.140 cm), N is the number of complete convective cells (marginal cells are excluded).

l (cm)	12.5	9.2	8.0	7.3	6.4	4.7	2.9
Γ	82	60	52	42	32	19	13
N	530	252	195	160	110	57	21

the stability region near the threshold.¹⁸⁻²⁰ However, the number of works devoted to BM convection is considerably lower than that devoted to RB. As far as we know, no work, either theoretical or experimental, has been published on the wavelength-selection problem for this instability.

Our goal in the present work is to study experimentally the influence of the aspect ratio Γ and of the distance to the threshold ϵ [defined in BM convection by $\epsilon = (R - R_C)/R_C = (M - M_C)/M_C$ as justified in Ref. 5] on the selected wavelength. In Sec. II the measurement method is described. Experimental results and a comparison with those obtained in RB convection are presented in Sec. III. Conclusions are given in Sec. IV.

II. EXPERIMENTAL PROCEDURE

The general characteristics of the experimental setup have already been published.²¹ The fluid used is a silicon oil (Rhodorsil 47V100) which has a viscosity of 1 P ($P=880$) at 25°C.

For the present work seven regular hexagonal containers are used to study the influence of the aspect ratio Γ on λ . Hexagonal vessels are used, because it has been observed²² that this geometrical form induces a minimum disorder. The aspect ratio Γ is defined as $\Gamma = \sqrt{S/d}$, where S is the surface of each of these vessels, the characteristics of which are gathered in Table I, for a liquid depth $d=0.140$ cm; N stands for the number of complete

convective cells in the vessel (the cells in contact with the walls are excluded because they are incomplete).

In the case of a high aspect ratio ($\Gamma \approx 85$), a square and a circular vessel are also used to find out what influence the form has on wavelength variations. In all cases the walls are made of Plexiglass, except for the circular one which is made of glass. (The thermal conductivity of glass is of the same order of magnitude as the Plexiglass.)

To study variations of λ versus ϵ , measurements have been made in the hexagonal vessel with a side length $l=12.5$ cm for two liquid depths, $d_1=0.162$ cm and $d_2=0.407$ cm, that correspond to aspect ratios $\Gamma_1=71.6$ and $\Gamma_2=28.5$, respectively. These two values are selected because for a shallow pool (i.e., for d_1) surface-tension effects prevail, while for thicker layers (for d_2 , for instance) buoyancy forces dominate the surface-tension ones.²³

For each experiment ϵ is fixed (in practice it is the mean-vertical temperature difference). Then the liquid depth and the two temperatures of the upper T_u and T_l lower surfaces are measured, respectively, with a sensor and two thermocouples. As a consequence the convective structure is slightly perturbed in these places. Preliminary experiments showed that a steady regime is reached after only a few hours. So 12 hours, at least, after measuring d , T_u , and T_l , photographs of the fluid pattern [Fig. 1(a)] are taken every 15 min. Then they are digitalized using a Voronoi reconstruction with a PDP 11 computer [Fig. 1(b)]. From this information the average distance r be-

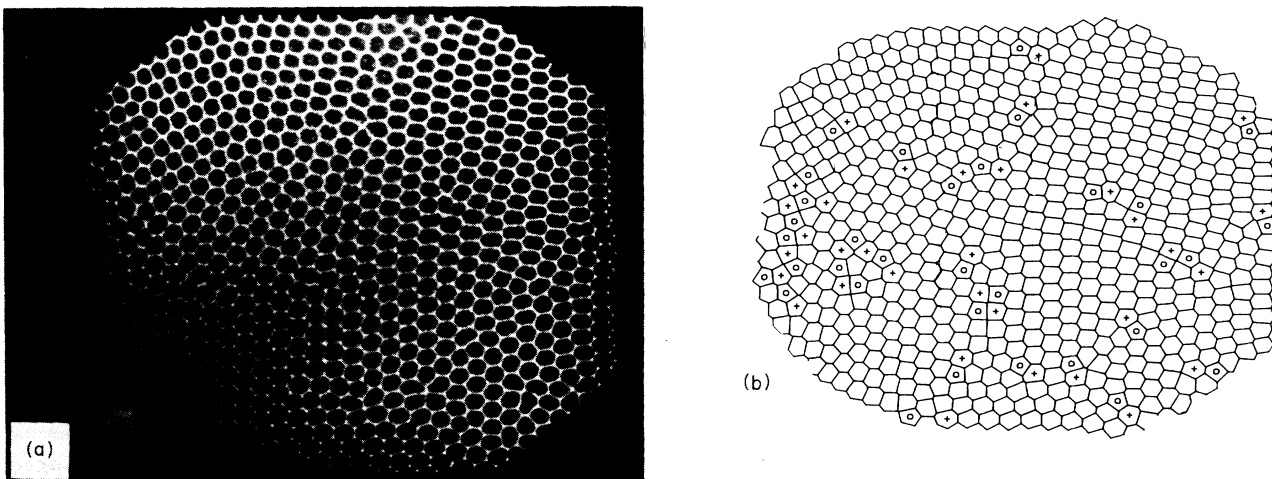


FIG. 1. Bénard-Marangoni convective structure for $\epsilon=0.5$. (a) Photograph of the pattern, (b) cell boundaries of (a) reconstructed by a computer program from the experimental positions of cell centers. The marginal cells are not taken into account. +, heptagonal cells; o, pentagonal cells.

tween neighboring cell centers, related to the wavelength λ through the relation $r = 2\lambda\sqrt{3}$, can be calculated. In this calculation we do not take into account the defects (pentagon-heptagon, "flower" defect, etc.²⁴) but only the regular or irregular hexagonal cells.

III. EXPERIMENTAL RESULTS: COMPARISON WITH RB CONVECTION

Taking photographs for 12 hours or so, we have observed that λ fluctuates randomly around a fixed value in all the considered cases. This phenomenon is related to the structural defects always existing in the pattern that evolve with time and provoke local variations on the hexagons. The amplitude of these fluctuations does not exceed 2%. The main results are summarized in the following.

A. Influence of the aspect ratio

For this experience the seven vessels (Table I) are filled with a liquid to a depth $d_1 = 0.140$ cm. The distance to the threshold is fixed at $\epsilon = 0.05$.

The main results can be seen in Fig. 2. The dimensionless wavelength $\lambda = \lambda_x/d$ increases for slow Γ until it reaches a limiting value for an aspect ratio about $\Gamma = 70$. This limit is $\lambda = 3.01$, which corresponds to $k = 2.08$ which is very close to the value obtained by the linear theory ($k = 2.1$).

For another depth $d = 0.162$ cm, the wavelength limit ($\lambda = 2.96$ corresponding to $k = 2.12$) for high aspect ratio ($\Gamma = 72.5$) is in good agreement with the preceding one taking into account the experimental uncertainties. So beyond the value $\Gamma \approx 70$, the liquid layer can be considered as an infinite layer.

In circular ($\Gamma = 88$) and square ($\Gamma = 85$) big boxes and for the same distance to the threshold $\epsilon = 0.05$, λ is 3.01 and only shows a small discrepancy (less than 2%) with the value found for a hexagonal container ($\lambda = 2.98$) with a similar aspect ratio ($\Gamma = 83$). Therefore, as expected, for high aspect ratios the particular form of the walls seems to have no significant influence on the wavelength-selection mechanism.

B. Influence of the distance to the threshold

The main results are quoted in Fig. 3 from which it is

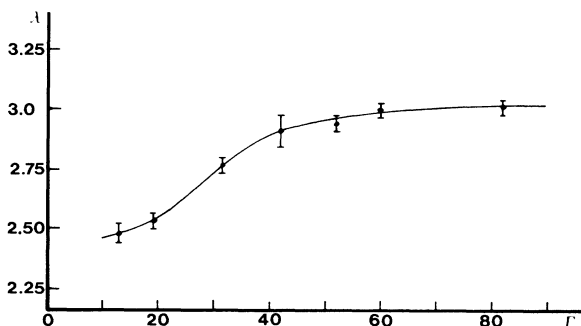


FIG. 2. Variation of the dimensionless wavelength λ as a function of the aspect ratio Γ , in a hexagonal container, for $\epsilon = 0.05$.

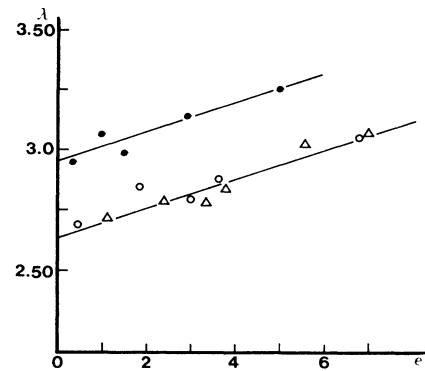


FIG. 3. Variation of the dimensionless wavelength λ as a function of the distance to the threshold ϵ , in a hexagonal container. Layer depth: ●, 0.162 cm ($\Gamma = 72$); △, ○, 0.407 cm ($\Gamma = 29$).

obvious that, in the considered range, λ increases with ϵ . Beyond $\epsilon \approx 7$ the number of defects becomes important ($> 45\%$) and the motions are rather erratic. Therefore, it is no longer feasible to talk about the wavelength of a hexagonal pattern.

For the two liquid depths under consideration, λ increases linearly with ϵ . The difference in the instability mechanism (surface tension prevailing for d_1 ; buoyancy for d_2) does not influence the corresponding slope, which has in both cases the same value $d\lambda/d\epsilon = 0.06$. It can be noticed that this is of the order of magnitude of the value $d\lambda/d\epsilon = 0.1$ (Refs. 13 and 14) obtained for roll patterns in RB convection.

Extrapolation to $\epsilon \rightarrow 0$ gives for Γ_1 and Γ_2 , $\lambda_1 = 2.96$ and $\lambda_2 = 2.64$ corresponding to wave numbers $k_1 = 2.12$ and $k_2 = 2.37$, which are in good agreement with the results given by Pantaloni *et al.*²⁵

For fixed vessels, a change in d leads to changes in Γ and in the Biot number $L = hd$ (where h accounts for the heat transport across the free surface) and, as seen in this work, it also changes the value of λ at the threshold (Table II).

When d increases in a fixed vessel, Γ diminishes, and, when Γ is below 70, wave numbers obtained in experiments must be higher than those found in linear analysis for infinite vessels. This fact could explain the apparent disagreement between linear calculations and some experimental results of Pantaloni *et al.*²⁵ obtained in circular containers with small aspect ratios (Table II). In the present study we have obtained $\lambda = 2.96$ for $\Gamma = 70$, while

TABLE II. Wavelengths for various liquid depths (d) at the threshold. L is the Biot number, k_c and k_e are the wave numbers, respectively, obtained from the linear theory (Ref. 3) and experimentally in a circular vessel (Ref. 25), Γ is the aspect ratio.

d (cm)	0.36	0.50	0.80
Γ	34.9	25.2	15.7
L	0.13	0.3	0.45
k_c	2.05	2.10	2.16
k_e	2.01	2.17	2.23

linear theory gives $\lambda=2.94$ for $L=0.45$ and an infinite vessel. This comparison also confirms that from a practical point of view containers with $\Gamma > 70$ may be considered as infinite.

C. Comparison with RB convective patterns

In all experiments described here the realized hexagonal pattern corresponds to a fixed wavelength (fluctuations apart) for fixed external conditions. So no hysteresis was observed between experiments in which λ was raised and those in which it was lowered. On the contrary, in RB convection, patterns of rolls with different λ seem to be stable for the same external conditions, and hysteresis phenomena between these λ 's might also occur.

These differences between RB and BM conventions can be explained by the fact that in our experiments the structure is slightly perturbed by the measurement of d and T but above all by the important differences between the pattern natures of these two instabilities.

The number of hexagonal cells filling a vessel is far greater than the number of rolls in a similar container. A new roll appearing in the pattern causes an abrupt and discontinuous variation of λ whereas the "birth" of a new cell in a hexagonal pattern only induces small, almost continuous changes on λ . These continuous variations of λ in hexagonal patterns are also favored by the elasticity of parietal cells (i.e., those incomplete cells in contact with side walls), which do not seem to have a well-defined shape. Those facts make hexagonal patterns less "rigid" and more adaptable than roll patterns. In this case it seems that the pattern chooses a well-defined mean λ (Γ

and ϵ being fixed) and no hysteretic changes can be seen (see also the conclusion in Ref. 26).

By means of a "thermal technique" developed recently,²⁶ hexagonal cells with an imposed side can be generated. The present work may be completed studying the wavelength evolution of such an imposed pattern (in big and in small boxes). We think that the corresponding final value of λ will coincide with that of spontaneous patterns considered in the present work.

IV. CONCLUSION

The aspect ratio Γ has a strong influence of the wavelength-selection mechanism in hexagonal patterns (BM convection). Two different regions can be distinguished. For small boxes the selected λ is a function of Γ , whereas for big ones ($\Gamma > 70$), λ reaches a saturation value that (for small ϵ) approaches the value given by the linear theory. As in RB convection, λ increases with ϵ . In the present case λ depends linearly on ϵ in the range under consideration.

ACKNOWLEDGMENTS

We should like to thank Dr. Occelli for his help in the process of digitalization. One of us (C.P.-G.) also thanks the Comision Asesora de Investigacion Cientifica y Tecnica (CAICYT) of the Spanish Government for partial financial support.

*Permanent address: Departament de Termologia, Facultat de Ciències, Universitat Autònoma de Barcelona, Bellaterra (Barcelona) Catalonia, Spain.

¹Cellular Structures in Instabilities, Vol. 210 of *Lecture Notes in Physics*, edited by J. F. Wesfreid and S. Zaleski (Springer, Berlin, 1984).

²S. Chandrasekhar, *Hydrodynamic and Hydromagnetic Stability* (Oxford University, London, 1961).

³D. A. Nield, *J. Fluid Mech.* **19**, 1941 (1964).

⁴H. Bénard, *Rev. Gen. Sci. Pur. Appl.* **11**, 1261 (1900).

⁵R. Occelli, E. Guazzelli, and J. Pantaloni, *J. Phys. Lett.* **44**, L597 (1983).

⁶For a review article see F. H. Busse, *Rep. Prog. Phys.* **41**, 1929 (1978).

⁷C. Perez-Garcia, in *Stability of Thermodynamics Systems*, Vol. 164 of *Lecture Notes in Physics*, edited by J. Casas-Vazquez and G. Lebon (Springer, Berlin, 1982).

⁸F. H. Busse and J. A. Whitehead, *J. Fluid Mech.* **47**, 305 (1971).

⁹A. Schlüter, F. Lortz, and F. M. Busse, *J. Fluid Mech.* **23**, 129 (1965).

¹⁰L. A. Segel, in *Nonequilibrium Thermodynamics: Variational Techniques and Stability*, edited by R. J. Donnelly et al. (University of Chicago, Chicago, 1966).

¹¹M. C. Cross, P. G. Daniels, P. C. Hohenberg, and E. D. Siggia, *Phys. Rev. Lett.* **45**, 898 (1980); *J. Fluid Mech.* **127**, 155 (1983).

¹²Y. Pomeau and P. Manneville, *Phys. Lett.* **75A**, 296 (1980).

¹³E. L. Koschmieder, *Adv. Chem. Phys.* **26**, 177 (1974).

¹⁴B. Martinet, P. Haldenwang, G. Labrosse, J. C. Payan, and R. Payan, *J. Phys. (Paris) Lett.* **43**, L161 (1982); *C. R. Acad. Sci.* **299**, 755 (1984).

¹⁵V. Croquette and A. Pocheau, in Ref. 1, p. 104.

¹⁶G. Ahlers, D. S. Cannell, and V. Steinberg, *Phys. Rev. Lett.* **54**, 1373 (1985); V. Steinberg, G. Ahlers, and D. S. Cannell, *Phys. Scr.* **T9**, 95 (1985).

¹⁷P. Kolodner, R. W. Walden, A. Passer, and C. M. Surko (unpublished).

¹⁸J. W. Scanlon and L. A. Segel, *J. Fluid Mech.* **30**, 149 (1967).

¹⁹S. Rosenblatt, S. H. Davis, and G. M. Homsy, *J. Fluid Mech.* **120**, 91 (1982).

²⁰A. Cloot and G. Lebon, *J. Fluid Mech.* **145**, 447 (1984).

²¹P. Cerisier, J. Pantaloni, G. Finiels, and R. Amalric, *J. Appl. Opt.* **21**, 2153 (1982).

²²C. Jamond, Ph.D. thesis, University of Provence, Marseilles, 1985.

²³P. Cerisier, C. Jamond, J. Pantaloni, and J. C. Charmet, *J. Phys. (Paris)* **45**, 405 (1984); C. Perez-Garcia, J. Pantaloni, R. Occelli, and P. Cerisier, *ibid.* **46**, 405 (1985).

²⁴P. Cerisier and J. Pantaloni, in Ref. 1, p. 197.

²⁵J. Pantaloni, R. Bailleux, J. Salan, and M. G. Velarde, *J. Non-Equilib. Thermodyn.* **4**, 201 (1979).

²⁶P. Cerisier, C. Perez-Garcia, C. Jamond, and J. Pantaloni, *Phys. Lett.* **112A**, 366 (1985).

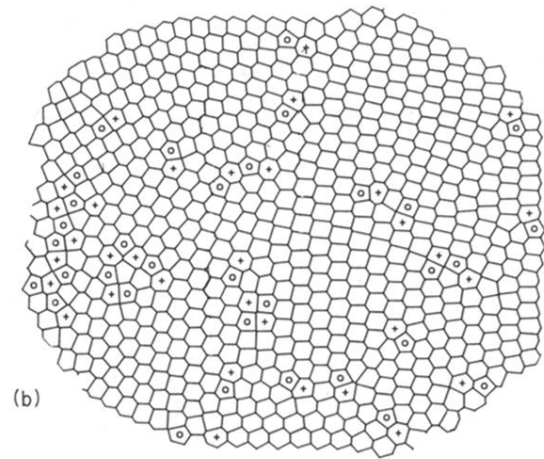
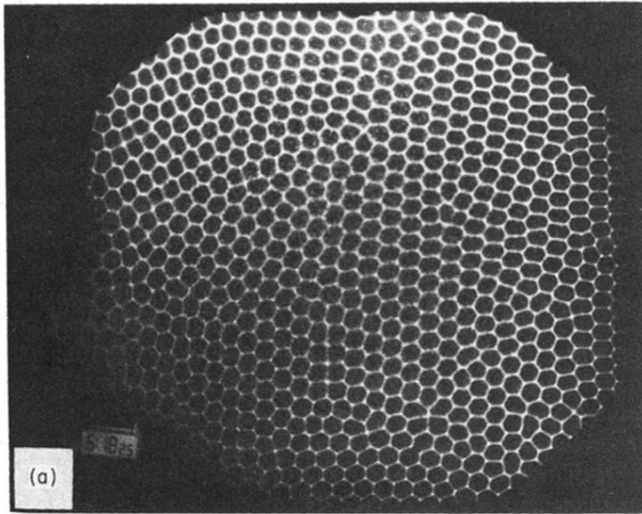


FIG. 1. Bénard-Marangoni convective structure for $\epsilon=0.5$. (a) Photograph of the pattern, (b) cell boundaries of (a) reconstructed by a computer program from the experimental positions of cell centers. The marginal cells are not taken into account. +, heptagonal cells; \circ , pentagonal cells.